A Metropolitan Wind Resource Assessment for Bangkok, Thailand Part 1: Wind Resource Mapping

Carina P. Paton[1,2] and Kasemsan Manomaiphiboon[1,2,*]

[1]The Joint Graduate School of Energy and Environment (JGSEE), King Mongkut's University of Technology Thonburi (KMUTT), Bangkok
[2]Center for Energy Technology and Environment, Ministry of Education, Thailand
126 Prachautit Rd., Bangmod, Tungkru, Bangkok 10140 Thailand
Tel: +66 2 470 7331, Fax: +66 2 470 7337
*Corresponding author. E-mail: kasemsan_m@jgsee.kmutt.ac.th

Abstract: Increased awareness of wind energy in Thailand has resulted in growing numbers of wind turbine installations in and around Bangkok province, the capital. However, little is known about the wind resource and its variation across the province. To address this, a two-part assessment was conducted, the first of which is described here: the development of a set of 1-km resolution wind resource maps at multiple heights (up to 300 m above ground level) using atmospheric modeling that was enhanced with satellite-derived land-related data to better resolve winds over urban spatial zones. Simulated wind resource maps show the annual wind resource within 100 m of the ground is poorest over the city center (<125 W m^{-2} at 100 m) and strongest in the southwest coastal area (up to 200 W m^{-2}). Wind resource becomes stronger with height, and at heights of 200-300 m and above it varies little across the province (200-300 W m^{-2}). The results found here provide input for the second paper, in which the overall technical wind resource potential is estimated for Bangkok in terms of electricity generation using geographical information system (GIS) analysis.

Keywords: Wind energy; spatial and temporal variations, atmospheric modeling; urban zones; Bangkok.

1. Introduction

The Thai Government is promoting wind among other forms of alternative energy to meet ever-increasing energy consumption that is predominantly supplied by fossil fuels [1-2]. Past and ongoing wind resource studies in Thailand range from meso-scale wind mapping over the entire country to micro-siting over limited areas. These studies found that enhanced wind resource exists in the western mountain ranges, southern coastlines, and the eastern edge of the Korat Plateau in the northeast [3-7]. One recent study supports local resident and wind energy community suspicion that moderate wind resource exists in the central region along the coast adjacent to the Gulf of Thailand [6]. This area includes Bangkok, Thailand's capital and the most populated and developed province (Figure 1), where three prevailing wind directions occur annually: the northeast monsoon (from mid-October to mid-February), the southerly summer kite winds (from mid-February to mid-May), and the southwest monsoon (from mid-May to mid-October).

To the best of the authors' knowledge, no previous wind resource assessments focus on a substantially urbanized area in Thailand. Recently emerging standalone and rooftop wind turbines in and around Bangkok tend to be unsystematically planned and installed across the province due to a lack of accurate and reliable wind information. The purpose of the study is to increase the existing but limited knowledge of and reduce the uncertainty in Bangkok's wind resource through 1-km-resolution wind resource mapping at multiple heights up to 300 m above ground level

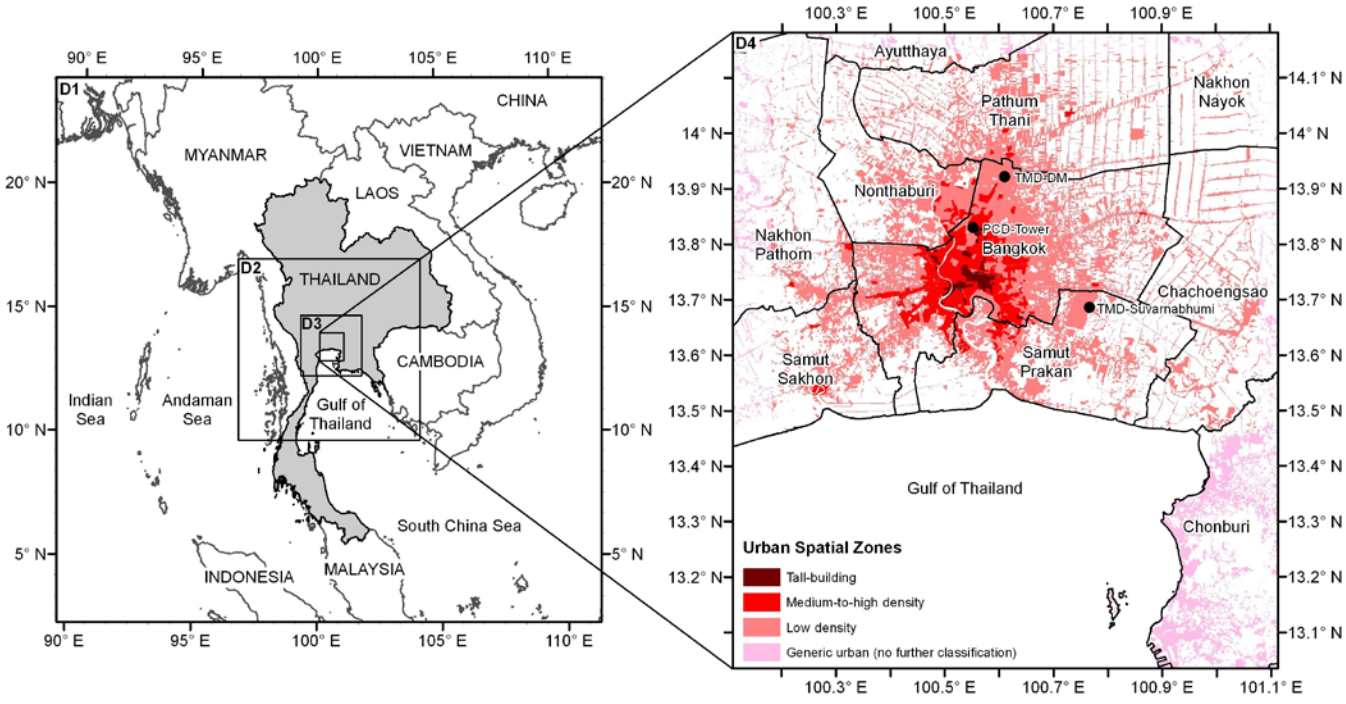

Figure 1. Modeling domains and urban spatial zones in Bangkok and its vicinity.

(AGL) as the height of the tallest building. In general, a spatial resolution of 1-3 km can be considered adequate in characterizing winds at an urban-zone scale (as opposed to a very local or fine scale, e.g., street or building scale), which is the intended scope of this study. It is hoped that the resulting maps from this effort could provide better understanding of Bangkok's overall wind resource and its characteristics, and be useful for wind energy planning.

2. Experimental

Several methods to estimate wind resource exist [8]; these include direct wind measurement, modeling, and combinations of the two. Wind data are collected at a number of surface meteorological stations in Bangkok, but according to our site surveys nearly all stations have limited measurement heights (~10 m or lower) and are also improperly situated for wind monitoring (particularly, affected or interfered by nearby objects or structures). Thus, to examine Bangkok's climate and validate model results in this study we only use data from suitably located stations (Figure 1): the 100-m meteorological tower of the Pollution Control Department (hereafter, PCD-Tower) that was located in Bangkok, and the surface station of the Thai Meteorological Department at Don Muang Airport (hereafter, TMD-DM). The TMD monitoring station at Suvarnabhumi Airport in Samut Prakarn province (to the east of Bangkok) is also considered suitably sited but it started operation in January 2008, which is after our study year (here, 2007).

Here, hourly gridded meteorological fields over the province and its vicinity were simulated using the Pennsylvania State University/National Center for Atmospheric Research mesoscale atmospheric model MM5 (version 3.7) [9]. It was an accessible model with which we were already familiar, and it is widely used in air quality and meteorological research areas [10-11]. It should be noted that although physics options provided in the standard MM5 model applied here do not account explicitly for urban physics (as do more recent atmospheric models [12-13]), we attempted to enhance our MM5 modeling using satellite-derived land-related data.

Four one-way nested modeling domains were employed with horizontal grid resolutions of 27 km, 9 km, 3 km and 1 km (Figure 1). As seen, the outermost domain (D1) covers most of mainland Southeast Asia, while the innermost domain (D4) spans 108 km east-to-west and 126 km north-to-south, encompassing the entire Bangkok province and its vicinity. Each modeling domain has 32 vertical layers, with 16 within the lowest 1.5 km and the top layer at 100 mb.

To improve urban surface heterogeneity in the modeling, we reclassified the 200+ categories in the high-resolution (<50 m) land cover data developed by the Thai Land Development to the default 24-category classification in MM5 [14], combined it with the 1-km resolution Global Land Cover Map for the Year 2000 [15] for land outside Thailand, and then re-gridded to the four modeling grids. Areal coverage of some land cover categories changed significantly after modification (Figure 2): forest area in D1 reduced from 47% of land area in default MM5 land cover data to 31% in our improved land cover, grassland area in D1 increased from 5% to 23%, and urban land area increased significantly in D4, from 4% to 33%. Because the terrain of Bangkok and its vicinity is low lying and mostly uniform (<10 m above mean sea level), the only complex feature is the built environment, which covers 64% of land area in Bangkok. To account for this, similar to Civerolo et al. [10] we split the single default urban category in MM5 into three urban spatial zones over Bangkok and its vicinity and used them in D3 and D4 (Figure 1 and Table 1): tall-building, medium-to-high density, and low density. Zone demarcation was manually derived through field surveys, photographs, and satellite images. Aerodynamic surface roughness length remained at the default MM5 values, except for the urban spatial zones which were assigned the values presented in Table 1.

Table 1. Three urban spatial zones in Bangkok and their surface roughness lengths.

Zone	Description	Example[a]	Surface roughness length (m)
Tall-building	Clusters of tall buildings, with long shadows clearly visible on satellite imagery [16].		3.0[b]
Medium-to-high density	Closely-spaced buildings of mixed roof area and height (1 to ~8 floors). Commercial, medium-density facilities, and multi-household residential, minimal building shadows on satellite imagery.		1.5[c]
Low density	Detached single-household residential of 1-2 floors, industrial and large commercial with large roof areas, and low-density facilities.		0.5[c]

[a] Taken during 2010-2011
[b] Based on Takahashi et al., and Al-Jiboori and Hu [17-18]
[c] Based on Oke, and Grimmond and Oke [19-20]

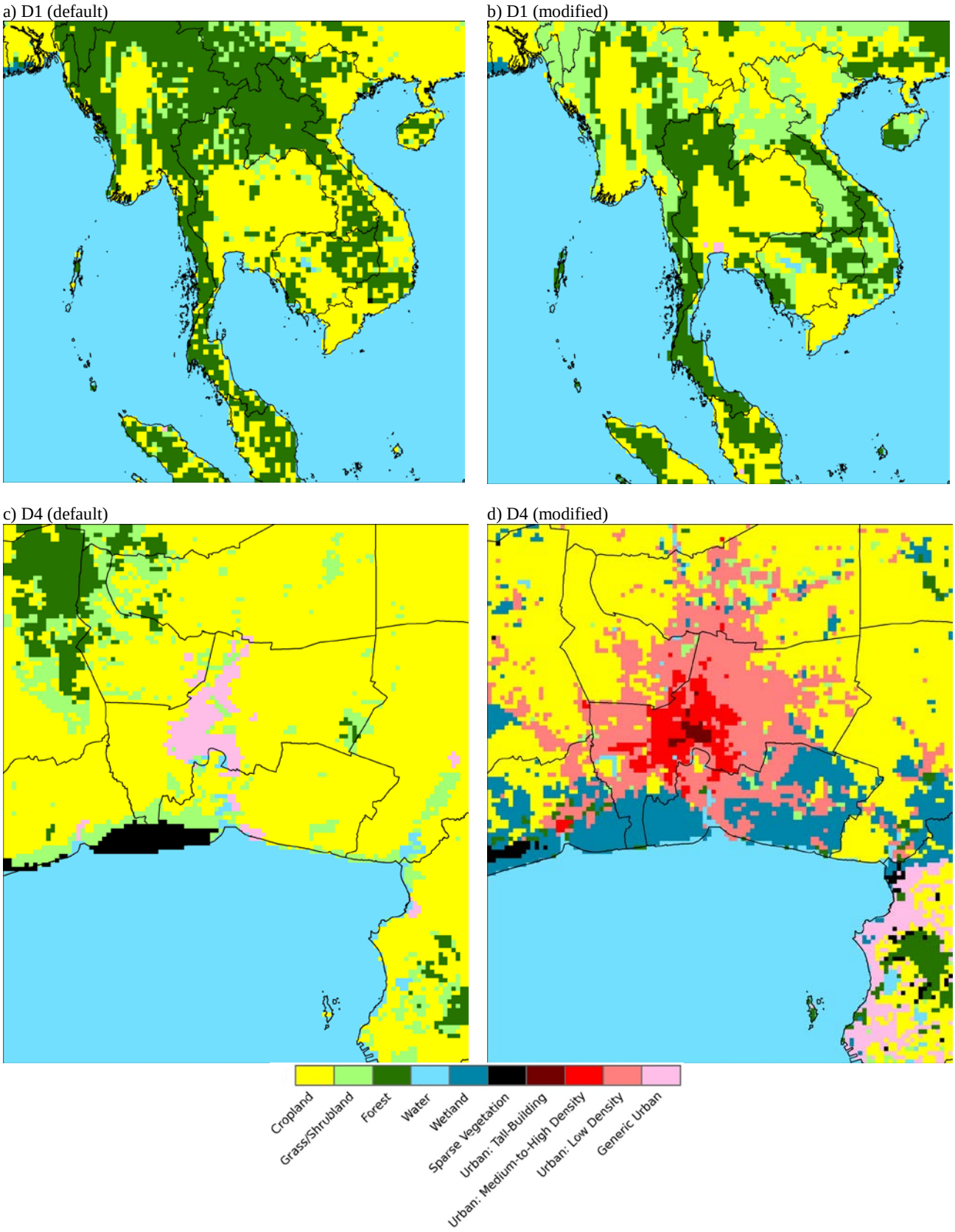

Figure 2. Default (a, c) and modified (b, d) land cover over the outermost modeling domain, D1, and the innermost domain, D4.

We modified monthly vegetation fraction f_g for each grid cell in a given month using monthly 1-km resolution normalized difference vegetation index (*NDVI*) from a MODIS satellite vegetation indices product (MOD13A3) and the method of Gutman and Ignotov [21],

$$f_g = \frac{NDVI - NDVI_o}{NDVI_\infty - NDVI_o}, \quad (1)$$

where subscripts o and ∞ denote bare soil and dense green vegetation, respectively, set here to be the 5th and 95th percentiles of *NDVI* of all grid cells in the month. The resulting maps were then re-gridded to each modeling domain (examples are shown in Figure 3). These appear to match well with satellite imagery [16] and show substantial improvement in spatial distribution in comparison to MM5-default vegetation fraction (not shown).

Similarly to de Foy et al. [13], we derived seasonal surface albedo parameters for each land cover category, representative of the entire region covered by the modeling, from a 16-day, 1-km resolution MODIS albedo product (MCD43B3). We converted the 16-day diffuse "white-sky" albedo ($\rho_{white\text{-}sky}$) and directional "black-sky" albedo ($\rho_{black\text{-}sky}$) to monthly resolutions using simple weighted averaging, and then computed actual "blue-sky" albedo ($\rho_{blue\text{-}sky}$) using

$$\rho_{blue-sky} = f_D \rho_{white-sky} + (1 - f_D)\rho_{black-sky}, \quad (2)$$

where f_D is the monthly average diffuse fraction (of global irradiation). The resulting monthly blue-sky albedo data was averaged for each season over all grid cells in each individual land cover category, and used as model input (see Table 2).

Data for initial and boundary atmospheric conditions input to the modeling include: global reanalysis data from the Japan Meteorological Agency Climate Data Assimilation System—which integrates various forms of data with relatively intensive data incorporation for East Asia and the tropics—for 3-dimentional atmospheric states (1.25° resolution) [22]; the Real-Time Global Sea Surface Temperature reanalysis data (0.5° resolution) [23]; and the National Centers for Environmental Prediction Global Final reanalysis data (1° resolution) to supply adequate multi-layered sub-surface soil moisture and temperature data [24].

Table 2. Default and modified albedo values by land cover and season.

USGS Land Cover	Description	Default		Modified[a]	
		Summer	Winter	Summer	Winter
1	Generic urban	0.15	0.15	0.14	0.14
2	Dryland cropland and pasture	0.17	0.23	0.16	0.16
3	Irrigated cropland and pasture	0.18	0.23	0.14	0.15
4	Mixed dry/irrigated cropland and pasture	0.18	0.23	(0.18)	(0.23)
5	Cropland/grassland mosaic	0.18	0.23	0.14	0.13
6	Cropland/woodland mosaic	0.16	0.20	0.14	0.13
7	Grassland	0.19	0.23	0.14	0.14
8	Shrubland	0.22	0.25	0.14	0.13
9	Mixed shrubland/grassland	0.20	0.24	0.14	0.13
10	Savanna	0.20	0.20	(0.20)	(0.20)
11	Deciduous broadleaf forest	0.16	0.17	0.15	0.13
12	Deciduous needleleaf forest	0.14	0.15	(0.14)	(0.15)
13	Evergreen broadleaf forest	0.12	0.12	0.14	0.13
14	Evergreen needleleaf forest	0.12	0.12	0.14	0.12
15	Mixed forest	0.13	0.14	0.14	0.14
16	Water bodies	0.08	0.08	(0.08)	(0.08)
17	Herbaceous wetland	0.14	0.14	0.12	0.12
18	Wooded wetland	0.14	0.14	0.11	0.11
19	Barren or sparse vegetation	0.25	0.25	0.13	0.13
20	Herbaceous tundra	0.15	0.15	(0.15)	(0.15)
21	Wooden tundra	0.15	0.15	(0.15)	(0.15)
22	Mixed tundra	0.15	0.15	(0.15)	(0.15)
23	Bare ground or tundra	0.25	0.25	0.12	0.10
24	Snow or ice	0.55	0.70	(0.55)	(0.70)
25	No data	NA[b]	NA	NA	NA
26	Urban: tall-building	NA	NA	0.14	0.14
27	Urban: medium-to-high density	NA	NA	0.14	0.14
28	Urban: low density	NA	NA	0.14	0.14

[a] Values in parentheses are unmodified from default MM5 values
[b] NA: Not applicable

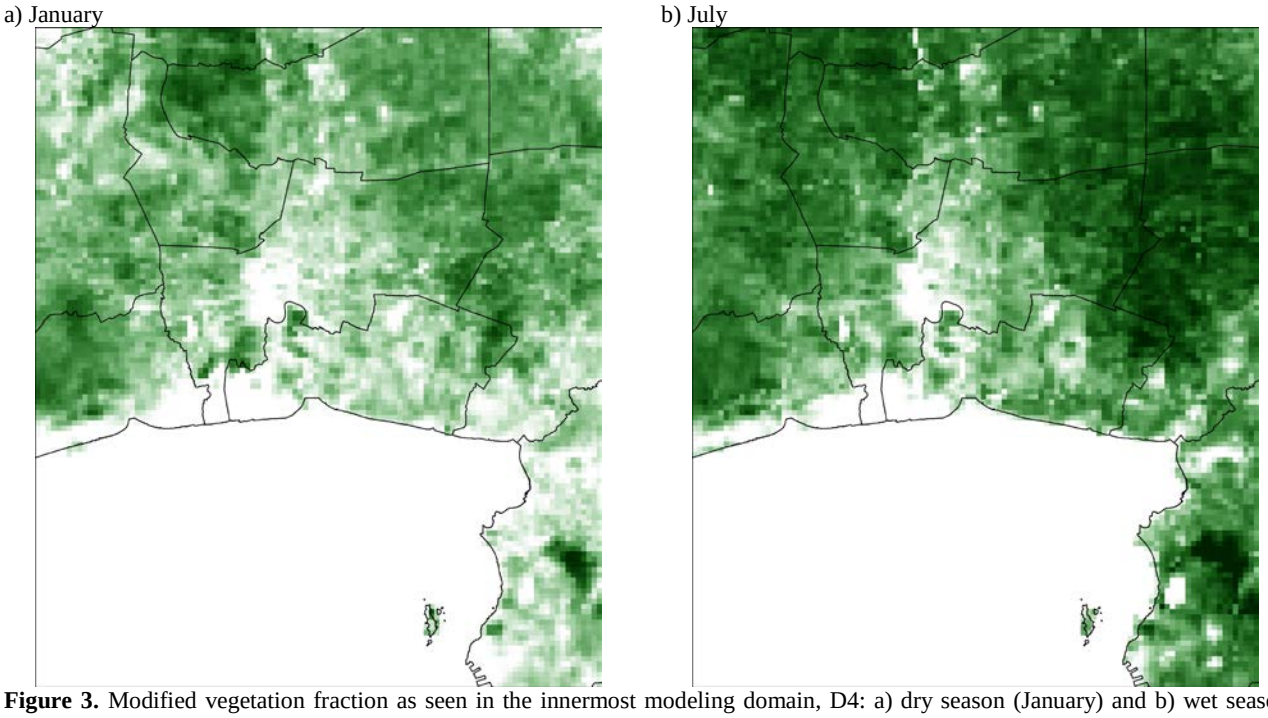

Figure 3. Modified vegetation fraction as seen in the innermost modeling domain, D4: a) dry season (January) and b) wet season (July). The degree of shading corresponds to that of vegetation fraction.

To select physics options, we followed Manomaiphiboon et al. [6] in performing several short-term sensitivity tests and comparing simulated wind speed and near-surface air temperature to observation data collected at PCD-Tower. From this, we selected a combination of the Grell cumulus parameterization scheme, Pleim-Chang planetary boundary layer scheme, and Pleim-Xiu land surface model for use in conjunction with simple ice explicit moisture, rapid radiative transfer model atmospheric radiation, and shallow convective options.

The full year of 2007 was selected for simulation here due primarily to our computational resource and observation data constraints. For this year, hourly wind data from PCD-Tower are nearly complete (with only <4% missing). Also, annual and seasonal mean wind speeds over Bangkok in 2007 (derived from PCD-Tower and routine upper air soundings sampled four times daily at 850 mb at the Thai Meteorological Department headquarters in southern central Bangkok) show no extreme deviations from their overall trends during 2000-2009. Furthermore, regional climatic conditions in this year were found to not be strongly affected by large scale perturbations (here, in terms of an El Niño Southern Oscillation index; details are not shown). Therefore, it is possible to use 2007 as a representative year for the study. Here, the model was run over the entire year of 2007 in individual eight-day episodes (i.e., reinitialized every eight days), discarding the first day of each as spin-up time. The reason we choose this running method was to avoid the large modeling drifts or errors as we experienced with longer episodes.

The wind speed and near-surface temperature prediction capability of the model was evaluated by comparing hourly values over the entire year from the simulation (S_h) and those from observed values at PCD-Tower (O_h) using the monthly and annual mean bias (*MB*) metric:

$$MB = \frac{1}{N}\sum_{h=1}^{N}(S_h - O_h), \quad (3)$$

where N is the number of data pairs. The model gave small-to-fair overestimates for wind speed, but overall performance may be considered acceptable for the purposes of wind resource mapping: At PCD-Tower (100 m AGL), monthly *MB* ranged from <0.1 to 2.8 m s^{-1} (with observed means of 2.9 to 5.1 m s^{-1}) and annual *MB* was 1.4 m s^{-1} (observed mean of 3.3 m s^{-1}). At TMD-DM (~10 m AGL), monthly *MB* ranged from 1.1 to 4.3 m s^{-1} (with observed means of 1.3 to 3.1 m s^{-1}) and annual *MB* was 2.1 m s^{-1} (observed mean of 2.3 m s^{-1}). In our opinion, the larger discrepancies seen at TMD-DM are possibly due to larger influence on winds by the surroundings of the near-surface wind monitoring station, and our confidence in its use is much less than in the PCD-Tower case. Seasonal directional wind patterns were well captured, being compatible with regional prevailing winds (see Section 3). Model performance was acceptable for near-surface temperature: At PCD-Tower, monthly *MB* was in the acceptable range of −2.0 to 0.5°C (observed means of 26.0 to 30.5°C) and annual *MB* was −1.0°C (observed mean of 28.3°C). At TMD-DM, monthly *MB* was in the range of −3.8 to 0.6°C (observed means of 27.3 to 30.9°C) and annual *MB* was −0.7°C (observed mean of 29.0°C).

Wind power density was calculated using hourly simulated wind speed, temperature, pressure, and relative humidity. Values for these variables were interpolated to desired heights from MM5 vertical levels using a cubic spline method. It is noted that relative humidity was used to account for air density dependency on moisture. Annual and three-monthly (DJF, MAM, JJA, and SON as sequential calendar months) mean wind power densities at a grid cell and height were derived from hourly data.

3. Results and Discussion

A number of 1-km resolution wind resource maps over Bangkok were generated for heights of 20 to 300 m AGL (Figures 4 and 5). Since the study is in context of energy, it is more appropriate to discuss wind power density rather than

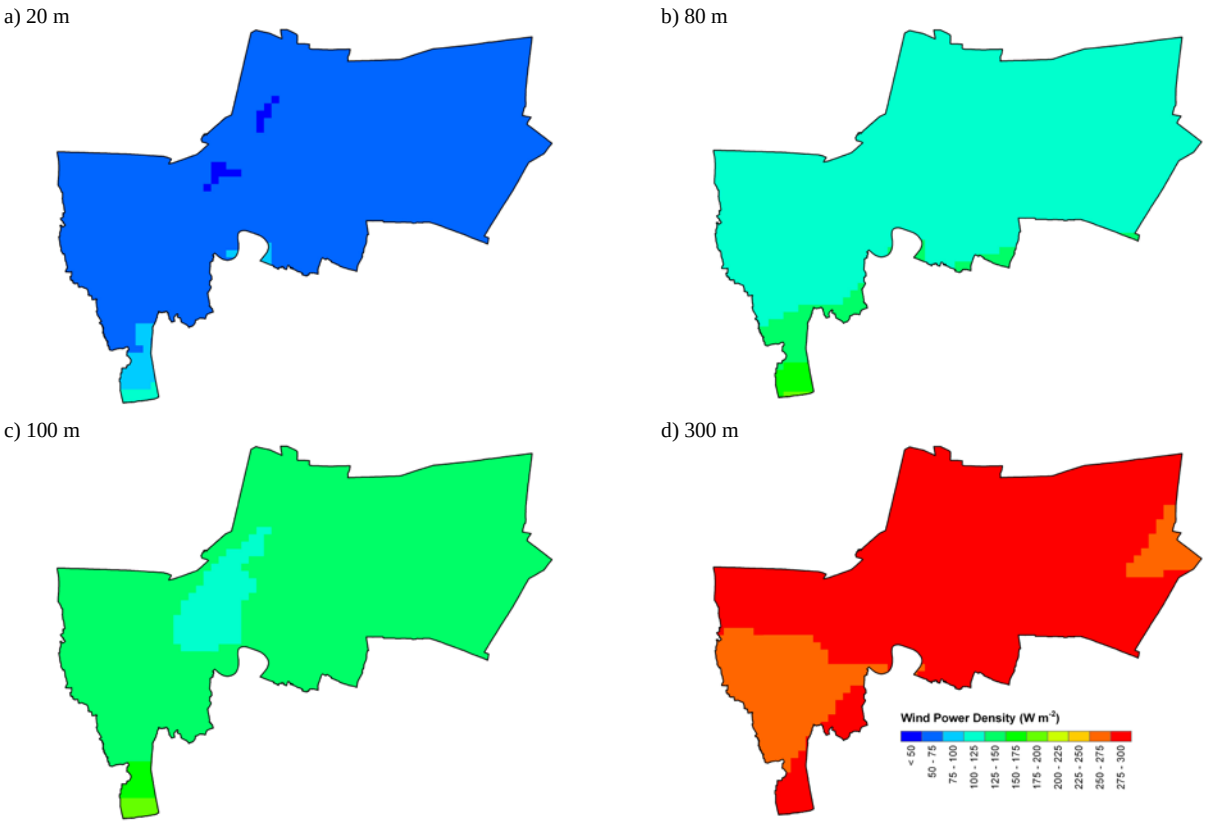

Figure 4. Maps of annual wind power density at 20 m, 80 m, 100 m, and 300 m above ground level.

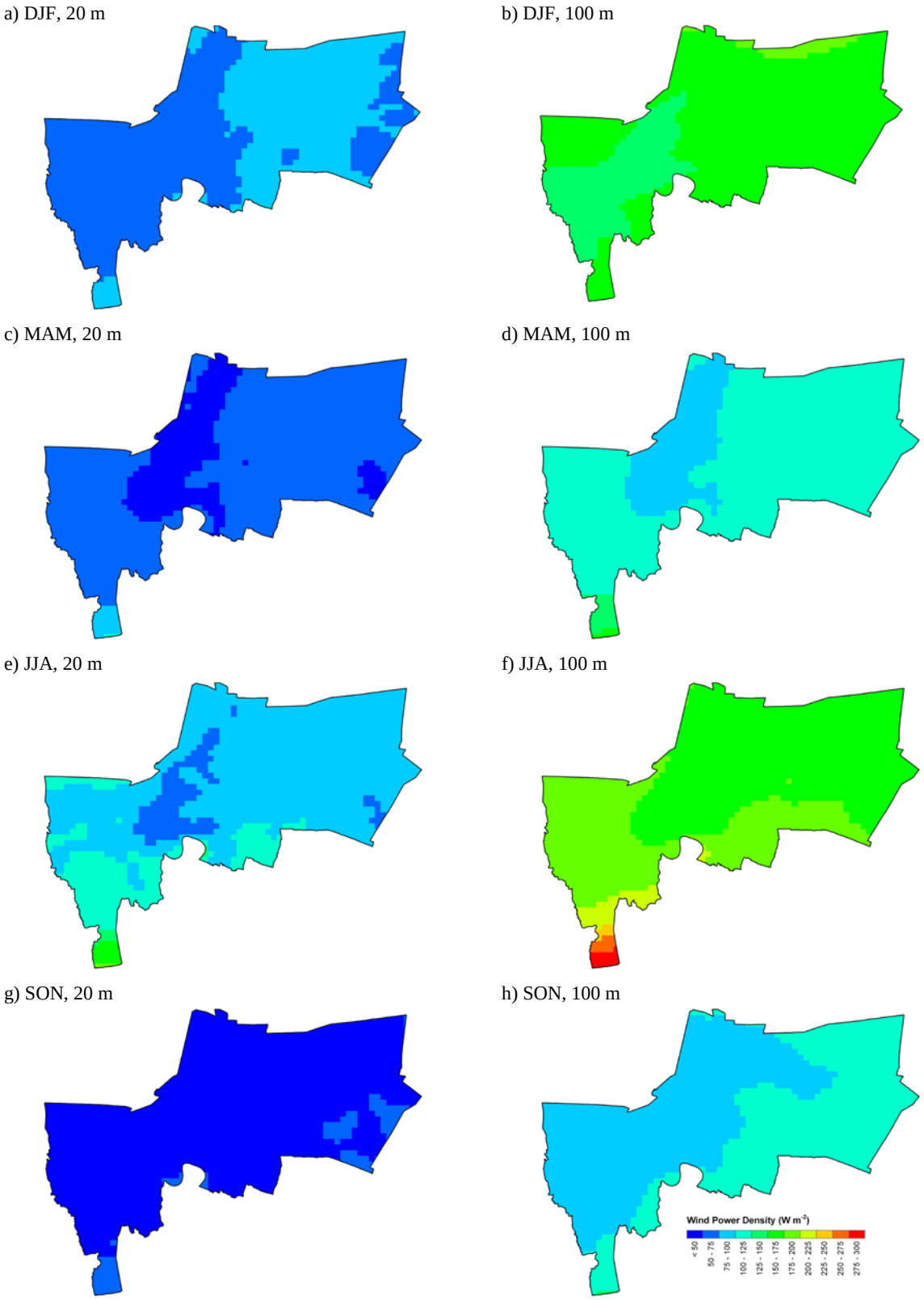

Figure 5. Maps of three-monthly wind power density at 20 m and 100 m above ground level.

wind speed. As seen in the figures, wind power density varies spatially (both horizontally and vertically) and temporally (here, three-monthly). Overall wind resource is relatively poor at 20 m (<50-125 W m^{-2}, Figure 4a) and improves at greater heights (100-200 W m^{-2} at 100 m and 200-300 W m^{-2} at 200-300 m, Figures 4c-d). For most parts of Bangkok, the vertical gradient of wind resource is relatively large for heights within about 100 m. Above 200 m it becomes small, implying no significantly increased benefit in terms of wind energy utilization beyond such heights. Also, at these heights, wind resource is somewhat uniform across the province (i.e., 200-250 W m^{-2} at 200 m). Wind resource in the city center, especially within 100 m, is lower than surrounding areas (i.e., as low as 50 W m^{-2} at 20 m and 125 W m^{-2} at 100 m), and this contrast is more evident in

the middle of the wet season (Figure 5e) when winds due to the southwest monsoon are strong in magnitude. This is due mainly to higher surface roughness in the city center than in the outskirts. The larger wind resource year round in southwest Bangkok (i.e., up to 125 W m^{-2} at 20 m and 200 W m^{-2} at 100 m, see Figure 4) is likely attributed to its proximity to the Gulf of Thailand, as winds lose power with distance inland due to surface friction. During June-August, wind strength peaks, especially near the coast (i.e., 175-200 W m^{-2} at 20 m and 275-300 W m^{-2} at 100 m, Figures 5e-f). In September-November, wind resource within 100 m is relatively homogeneous across the province and is the lowest among all periods (i.e., <75 W m^{-2} at 20 m and 75-125 W m^{-2} at 100 m, Figures 5g-h), which is reasonable since these months fall in the late wet season and the southwest-to-northeast monsoon transition. In December-February (Figures 5a-b), when the northeast monsoon prevails, wind resource within 100 m is higher over the upwind east side of the city and near the coast (at 20 m, 75-100 W m^{-2}), but is lower downwind (southwest) of the city (50-75 W m^{-2}). In the hot season (around March-May), the southerly summer kite winds that typically flow through the study area during this period approximately delineate the urbanized and non-urbanized portions of the city (seen at both 20 m and 100 m in Figures 5c-d).

We compared these results with those of previous works: World Bank (WB) and Department of Energy Development and Promotion (DEDP) studies from 2001 [4-5], and the Joint Graduate School of Energy and Environment (JGSEE) and Department of Alternative Energy Development and Efficiency (DEDE) studies from 2010 [6-7]. Stronger wind resource near the coast (in terms of overall average wind power density) given in this study is also seen in WB and JGSEE but is not apparent in DEDP and DEDE. Reduced wind power density over the city center is most visible in DEDP and JGSEE but it has a lesser spatial extent than in this study, possibly due to the enhanced representation of urban/built-up areas in the modeling in this study. For most parts of Bangkok, wind resource found here is about one-half of what is given in DEDP and JGSEE, but there is better agreement with JGSEE over the city center and its surroundings. This is not surprising because JGSEE also used Land Development Department land cover which has urban land cover over Bangkok larger than the default, but it did not incorporate our additional higher surface roughness zones which suppress wind speed. Increased wind resource in the wet season seen here is also apparent in JGSEE and DEDE.

4. Conclusions and Recommendations

A set of 1-km wind resource maps at multiple heights (up to 300 m AGL) was developed for Bangkok using atmospheric modeling that was enhanced with satellite-derived and other land-related information, in support of future wind energy utilization in Bangkok. On average, wind resource within 100 m is highest in southwest Bangkok near the coast (e.g., up to 125 W m^{-2} at 20 m and 200 W m^{-2} at 100 m) and poorest over and around the city center (e.g., <50 W m^{-2} at 20 m and 125 W m^{-2} at 100 m). Wind resource increases with height rapidly near the ground and varies little above 200 m, where wind resource becomes fairly uniform over most of the province (e.g., 200-250 W m^{-2} at 200 m), even over the city center, implying that rooftop and building integrated turbines could be attractive at those heights. Wind resource varies seasonally, being highest during June to August and lowest during September to November. The seasonally averaged wind directions appear to agree with regional prevailing winds (e.g., dry northeast monsoon, wet southwest monsoon, and kite winds).

The wind resource modeling employed here was intended to characterize winds at a city scale in support of the overall wind resource potential estimation, and the 1-km resolution used here is suitable given the uniform topography in and around Bangkok. To overcome the technical limitations in this study, we recommend the following for future modeling efforts: use of urban canopy treatment for mesoscale modeling, coupling of mesoscale modeling with turbulence modeling or computational fluid dynamics at a local or micro-scale for finer (<1 km) resolutions, and longer-term simulation to better understand inter-annual wind resource variability.

Acknowledgements

The authors sincerely thank the Pollution Control Department for tower data, the Thai Meteorological Department for upper air data, and the Land Development Department for land cover data over Thailand. The authors also thank the MM5 development and support teams, and the Japan Meteorological Agency and the National Centers for Environmental Prediction for providing reanalysis data. The MODIS satellite data are distributed by the Land Processes Distributed Active Archive Center, US Geological Survey, and global land cover data used is generously provided by EC-JRC. The authors received useful comments from Dr. RHB Exell and Dr. Boonrod Sajjakulnukit (JGSEE) and general assistance from members of the JGSEE Computational Laboratory, especially Phan Thanh Tung. We also thank Dr. Chumnong Sorapipatana (JGSEE) for his encouragement for the authors to carry out wind energy research at JGSEE. This work was financially supported mainly by JGSEE and the Thailand Research Fund (Grant No. RDG5050016) and partially by the Postgraduate Education and Research Development Office (Grant No. JGSEE/PROJECT/002-2011).

References

[1] Department of Alternative Energy Development and Efficiency (Ministry of Energy), *The Renewable and Alternative Energy Development Plan for 25 Percent in 10 Years (AEDP 20120-2021)*, Available online: http://www.dede.go.th/dede/images/stories/pdf/dede_aedp_2012_21.pdf [accessed 23 Sep 2012].

[2] Electricity Generating Authority of Thailand, *Summary of Thailand Power Development Plan 2010-2030* (2010) Report No. 912000-5305. Summary of plan by Ministry of Energy, Thailand, Available online: http://www.egat.go.th/en/images/stories/pdf/Report%20PDP2010-Apr2010_English.pdf [accessed 15 Apr 2011].

[3] Exell RHB, The wind energy potential of Thailand, *Sol. Energy* 35/1 (1985) 3-13.

[4] World Bank, *Wind Energy Resource Atlas of Southeast Asia* (2011) Prepared by TrueWind Solutions, LLC, New York, US, Available online: http://siteresources.worldbank.org/EXTEAPASTAE/Resources/wind_atlas_complete.pdf [accessed 27 Nov 2009].

[5] Department of Energy Development and Promotion (currently Department of Alternative Energy Development and Efficiency) (Ministry of Energy), *Wind Resource Assessment of Thailand* (2011) In Thai, with English abstract, Prepared by Fellow Engineers Consultants Co. Ltd., Thailand.

[6] Manomaiphiboon K, Prabamroong A, Chanprasert W, Pajpreeja N, Phan TT, *Dual Database System of Wind Resource for Thailand* (2010) Final report of project: Wind Resource Assessment using Advanced Atmospheric Modeling and GIS Analysis. Conducted by the Joint Graduate School of Energy and Environment (King Mongkut's University of Technology Thonburi). Available online: http://complabbkt.jgsee.kmutt.ac.th/wind_proj [accessed 18 Apr 2011].

[7] Department of Alternative Energy Development and Efficiency (Ministry of Energy), *Development of Wind Resource Maps for Thailand* (2010) Prepared by Solar Energy Research Laboratory, Department of Physics, Silpakorn University, Thailand.

[8] Landberg L, Myllerup L, Rathmann O, Lundtang Petersen E, Jørgensen BH, Badger J, Mortensen NG, Wind resource estimation – an overview, *Wind Energ.* 6 (2003) 261-271.

[9] Grell GA, Dudhia J, Stauffer DR, A *description of the fifth-generation Penn State/NCAR mesoscale model (MM5)* (1995) Available online: http://www.mmm.ucar.edu.mm5/documents/mm5-desc-doc.html.

[10] Civerolo K, Hogrefe C, Lynn B, Rosenthal J, Ku J-Y, Solecki W, Cox J, Small C, Rosenzweig C, Goldberg R, Knowlton K, Kinney P, Estimating the effects of increased urbanization on surface meteorology and ozone concentrations in the New York City metropolitan region, *Atmos. Environ.* 41/9 (2007) 1803-1818.

[11] de Foy B, Molina LT, Molina MJ, Satellite-derived land surface parameters for mesoscale modeling of the Mexico City basin, *Atmos. Chem. Phys.* 6/5 (2006) 1315-1330.

[12] Tewari MF, Chen F, Kusaka H, Miao S, *Coupled WRF/unified NOAH/urban-canopy modeling system* (2008) NCAR WRF Documentation.

[13] Kusaka H, Kondo H, Kikegawa F, Kimura F, A simple single-layer urban canopy model for atmospheric models: Comparison with multi-layer and slab models, *Bound.-Layer Meteorol.* 101/3 (2010) 329-358.

[14] Land Development Department (Ministry of Agriculture and Cooperatives), *Land Use and Land Cover Data for Thailand for the Years 2006-2007* (2007) [CD-ROM].

[15] European Commission, Joint Research Centre, *Global Land Cover 2000 database* (2003) Available online: http://gem.jrc.ec.europa.eu/products/glc2000/glc2000.php [accessed 3 Dec 2009].

[16] Google, *Google Earth* (Version 6.0.3.2197) [Software], Mountain View, CA. Available online: http://earth.google.com.

[17] Takahashi H, Nakamura Y, Suzuki H, Distribution of summertime intense rainfall frequency and the surface roughness in the Tokyo metropolitan area, *Proceedings of the Seventh International Conference on Urban Climate* (2009) Yokohama, Japan.

[18] Al-Jiboori MH, Hu F, Surface roughness around a 325-m meteorological tower and its effect on urban turbulence, *Adv. Atmos. Sci.* 22/4 (2005) 595-605.

[19] World Meteorological Organization, *Guide to Meteorological Instruments and Methods of Observation* (2008) WMO-No. 8, Seventh ed., Geneva.

[20] Grimmond CSB, Oke TR, Aerodynamic properties of urban areas derived from analysis of surface form, *J. Appl. Meteorol.* 38 (1999) 1262-1292.

[21] Gutman G, Ignatov A, Satellite-derived green vegetation fraction for the use in numerical weather prediction models, *Adv. Space Res.* 19/3 (1997) 477-480.

[22] Onogi K, Tsutsui J, Koide H, Sakamoto M, Kobayashi S, Hatsushika H, Matsumoto T, Yamazaki N, Kamahori H, Takahashi K, Kadokura S, Wada K, Kato K, Oyama R, Ose T, Mannoji N, Taira R, The JRA-25 reanalysis, *J. Meteorol. Soc. Jpn.* 85/3 (2007) 369-432.

[23] Gemmill W, Katz B, Li X, *Daily Real-Time Global Sea Surface Temperature – High Resolution Analysis at NOAA/NCEP* (2007).

[24] US National Centers for Environmental Prediction. *Updated daily: NCEP FNL Operational Model Global Tropospheric Analyses* (continuing from July 2009). Available online: http://dss.ucar.edu/datasets/ds083.2.

